Supplementary Information of

ENSO's Signature on the Estimation of Cloud Feedback to Global Warming

Huan Liu[1], Ilan Koren[1], Orit Altaratz[1]

[1]Department of Earth and Planetary Sciences, Weizmann Institute of Science, Rehovot, 76100, Israel

Supplementary Note 1

In the main text, we used ONI as a measure of ENSO because it is NOAA's primary indicator for monitoring the ENSO's oceanic signal and is widely used in ENSO-related studies. However, as a temperature-based index over the Niño 3.4 region, the ONI may miss other ENSO effects characterized by relatively weak temperature anomalies or those occurring over other regions (e.g., the Niño 1.2 region). Hence, to account for ONI's potential limitations in representing all ENSO effects and assess the sensitivity of our results, we analyze, in addition, six other ENSO indexes during our study period (01.1950–12.2021), including the Niño 1.2 index, the Niño 3 index, the Niño 4 index, the TNI, the SOI, and the BEST (see Secs. 2.1 and 2.2 in the main text).

Consistent with the results using ONI (Fig. 1c in the main text), all ENSO indexes show significant short-term trends, with a quick convergence towards very small values (Supplementary Figure 1). Generally, the corresponding trend becomes negligible for time windows longer than 30 y. Moreover, the R^2 values between these indexes and GMST (Supplementary Figure 2) decrease similarly to those between ONI and GMST (Fig. 1e in the main text). These findings suggest that the ONI-based statistics are robust and do not depend on the ENSO index type.

Supplementary Note 2

As discussed in the main text, unlike the EOF modes, the physical processes are not necessarily orthogonal. Hence, variations caused by one physical process can be expressed by several EOF modes, and signatures of different processes may merge into one mode, known as signal leakage. To test this issue for EOF1 of CF, CTT, and COD, Supplementary Figure 3 depicts the explained variance histogram of their EOF modes (228 per variable) and the corresponding correlations with the EOF1/PC1 (Fig. 2 in the main text).

For CF/CTT, the explained variance (Supplementary Figure 3a/1b) of EOF1 is significantly larger than that of the following modes. In addition, the correlations between EOF1 or PC1 and the following EOFs or PCs for CF/CTT (Supplementary Figure 3d/3e) are weak. These results indicate that the signal leakage is not a major concern when interpreting EOF1 of CF and CTT. However, for COD, the explained variance (Supplementary Figure 3c) of EOF1

(2.2 %) is only slightly larger than those of the following ones (e.g., 1.8 % for the second EOF and 1.6 % for the third EOF). Although weak correlations between its EOFs and PCs are also observed (Supplementary Figure 3f), we cannot exclude the signal leakage issue when interpreting EOF1 of the COD.

Supplementary Note 3

In the main text, we defined the "ENSO effect minimal time" for cloud feedback estimations by applying a threshold (1 W m^{-2} °C^{-1}) on the mean magnitude of the ENSO-related bias for each time window (i.e., $\overline{|bias|} < 1\,\mathrm{W}\,m^{-2}\,°\mathrm{C}^{-1}$; Fig. 7 in the main text). To assess the sensitivity of our results to this definition, we apply the same threshold but consider different statistics for determining the "ENSO effect minimal time". Instead of the mean, Supplementary Figure 4 and 5 use the maximal and minimal magnitude of the ENSO-related bias (i.e., $max(|bias|) < 1\,\mathrm{W}\,m^{-2}\,°\mathrm{C}^{-1}$ and $min(|bias|) < 1\,\mathrm{W}\,m^{-2}\,°\mathrm{C}^{-1}$) to examine the minimal time under extremely strong and weak ENSO conditions, respectively. In addition, Supplementary Figure 6 uses the standard deviation (σ) of the ENSO-related bias (i.e., $\overline{|bias|} + \sigma(|bias|) < 1\,\mathrm{W}\,m^{-2}\,°\mathrm{C}^{-1}$) to examine the uncertainty of the "ENSO effect minimal time", as defined in the main text.

As expected, for both methods, a much longer (shorter) minimal time is revealed globally under extremely strong (weak) ENSO conditions (Supplementary Figure 4 and 5). However, importantly, even when ENSO activities are extremely weak, for $\mathrm{Method}_{\mathrm{GMST}}$, most tropical regions hold an "ENSO effect minimal time" longer than 50 y (white shades in Supplementary Figure 5). This feature highlights again the need to decouple ENSO's signature when estimating the cloud feedback to global warming. Supplementary Figure 6 suggests a several-year uncertainty of the "ENSO effect minimal time" as defined in the main text.

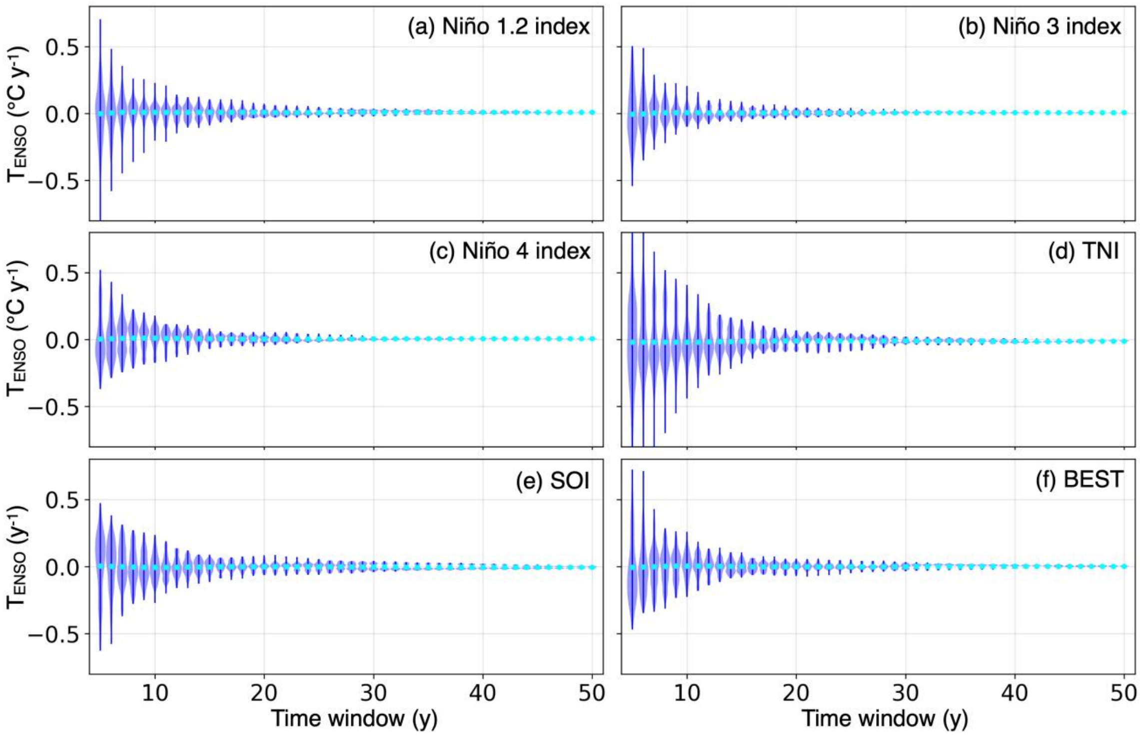

Supplementary Figure 1: The temporal trend violin plot (estimated by the OLS regression slope) for different ENSO indexes during 01.1950−12.2021, presented as a function of the time window (in intervals of 1 y). (a) The Niño 1.2 index, (b) the Niño 3 index, (c) the Niño 4 index, (d) the TNI, (e) the SOI, and (f) the BEST. Per time window, the vertical line marks the range (minimal to maximal); the shaded area represents the probability density; the cyan dots represent the mean value.

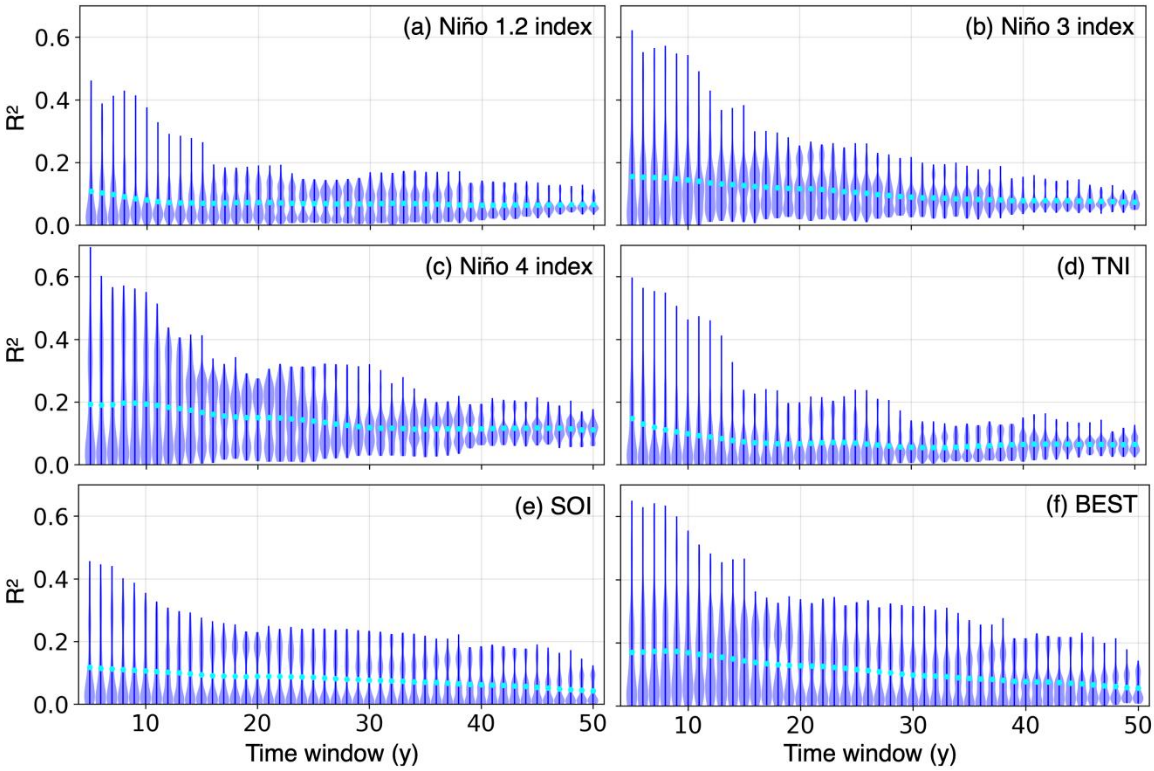

Supplementary Figure 2: The R^2 values violin plot (estimated by the square of Spearman's ρ) between different ENSO indexes and GMST during 01.1950–12.2021, presented as a function of the time window (in intervals of 1 y). (a) The Niño 1.2 index, (b) the Niño 3 index, (c) the Niño 4 index, (d) the TNI, (e) the SOI, and (f) the BEST. Per time window, the vertical line marks the range (minimal to maximal); the shaded area marks the probability density; the cyan dots represent the mean value.

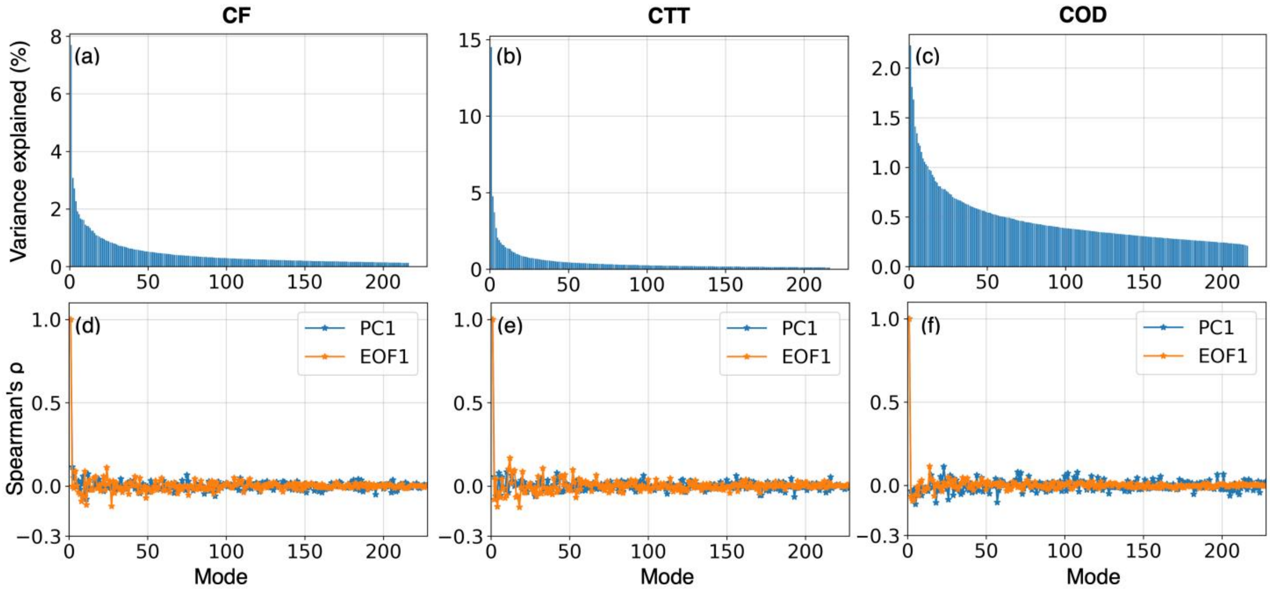

Supplementary Figure 3: A signal leakage test for EOF1 of the CF (left column), CTT (middle column), and COD (right column) during 12.2002−11.2021. (a−c) The explained variance (unit: %) of all EOFs and (d−f) correlations between the EOF1/PC1 and all EOFs/PCs (orange/blue dotted lines).

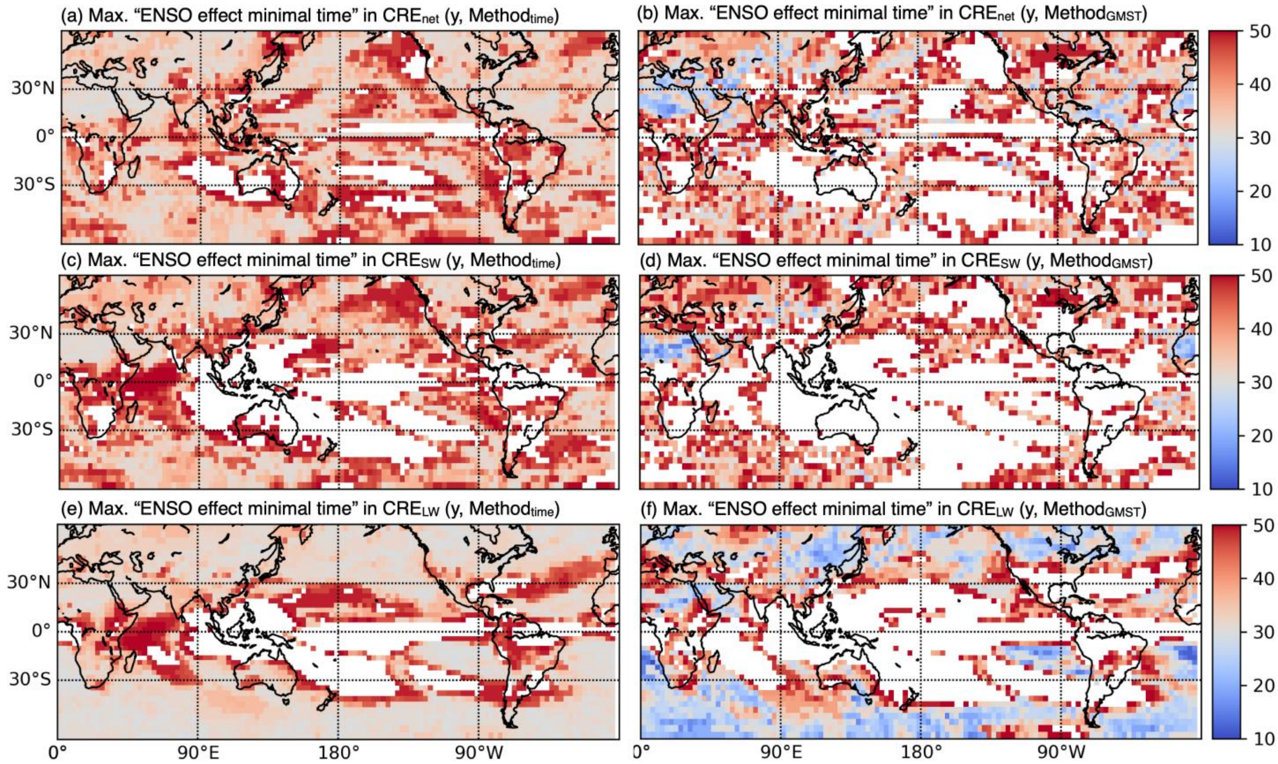

Supplementary Figure 4: The "ENSO effect minimal time" (unit: y), defined by the maximal magnitude of the ENSO-related bias in cloud feedback estimations during 01.1950–12.2021, estimated by $Method_{time}$ (left column) and $Method_{GMST}$ (right column). (a–b) CRE_{net}; (c–d) CRE_{SW}; and (e–f) CRE_{LW}. Areas with an "ENSO effect minimal time" longer than 50 y (beyond the maximal time window examined here) are marked in white.

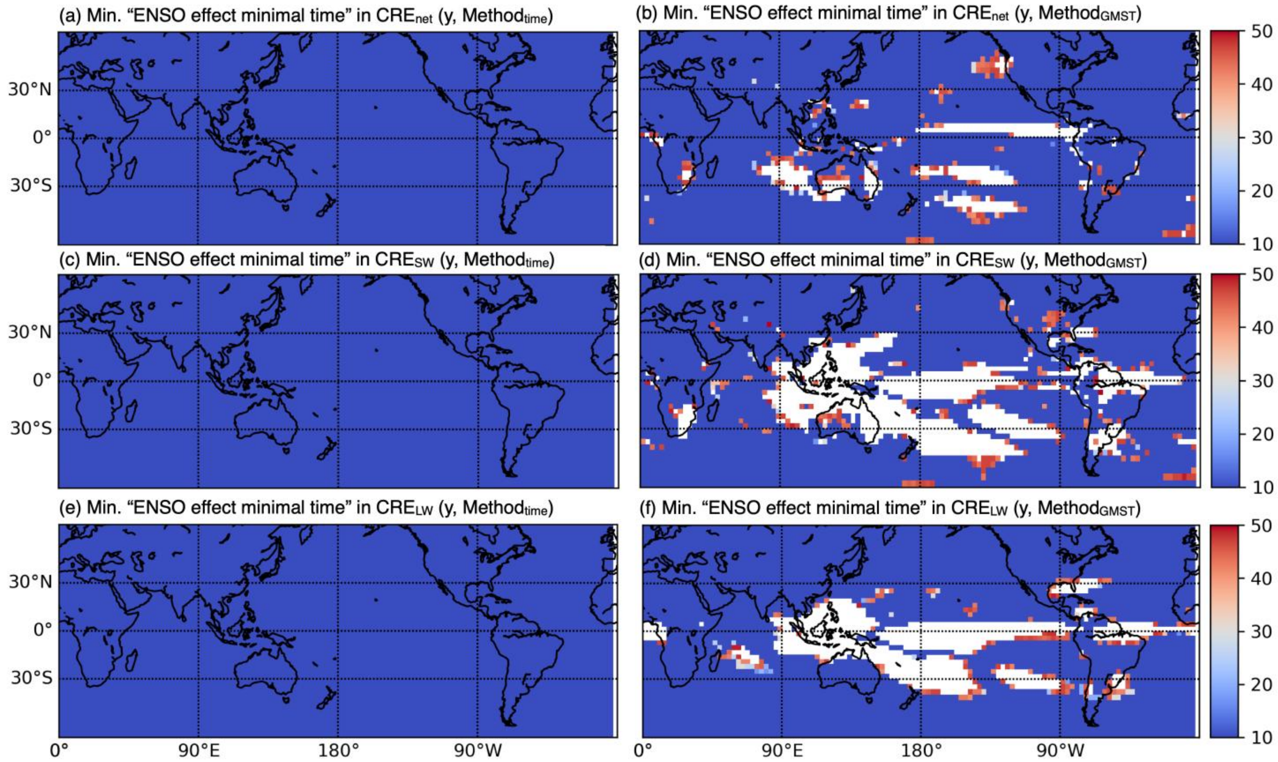

Supplementary Figure 5: The "ENSO effect minimal time" (unit: y), defined by the minimal magnitude of the ENSO-related bias, in cloud feedback estimations during 01.1950–12.2021, estimated by $Method_{time}$ (left column) and $Method_{GMST}$ (right column). (a–b) CRE_{net}; (c–d) CRE_{SW}; and (e–f) CRE_{LW}. Areas with an "ENSO effect minimal time" longer than 50 y (beyond the maximal time window examined here) are marked in white.

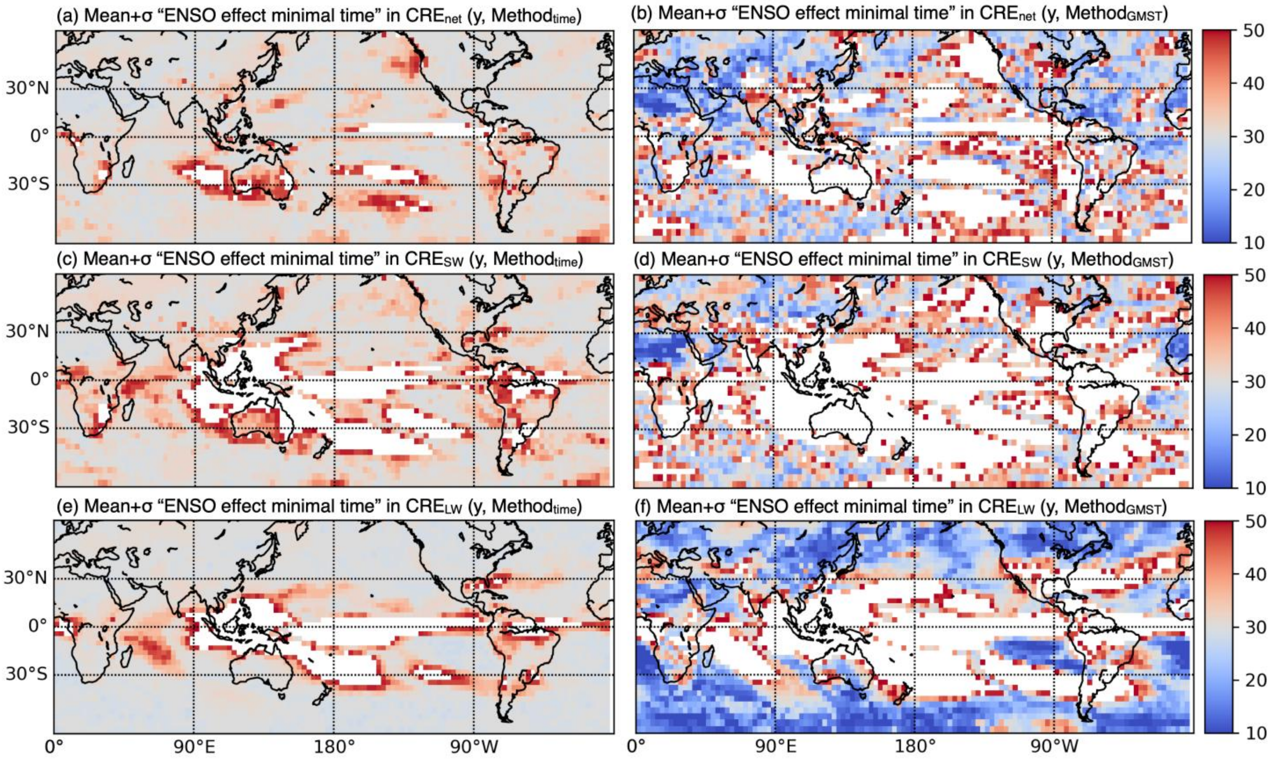

Supplementary Figure 6: The "ENSO effect minimal time" (unit: y), defined by the mean + σ of the ENSO-related bias, in cloud feedback estimations, during 01.1950–12.2021, estimated by $Method_{time}$ (left column) and $Method_{GMST}$ (right column). (a–b) CRE_{net}; (c–d) CRE_{SW}; and (e–f) CRE_{LW}. Areas with an "ENSO effect minimal time" longer than 50 y (beyond the maximal time window examined here) are marked in white.